

## Characterization of the melting transition in two dimensions at vanishing external pressure using molecular dynamics simulations

Daniel Asenjo,<sup>1,4</sup> Fernando Lund,<sup>1,\*</sup> Simón Poblete,<sup>2</sup> Rodrigo Soto,<sup>1</sup> and Marcos Sotomayor<sup>3</sup>

<sup>1</sup>*Departamento de Física and CIMAT, Facultad de Ciencias Físicas y Matemáticas, Universidad de Chile, Casilla 487-3, Santiago, Chile*

<sup>2</sup>*Max Planck Institute for Polymer Research, Ackermannweg 10, D-55128 Mainz, Germany*

<sup>3</sup>*Howard Hughes Medical Institute and Neurobiology Department, Harvard Medical School, Boston, Massachusetts 02115, USA*

<sup>4</sup>*Department of Chemistry, University of Cambridge, Lensfield Road, Cambridge CB2 1EW, United Kingdom*

(Received 23 January 2011; published 16 May 2011)

A molecular dynamics study of a two-dimensional system of particles interacting through a Lennard-Jones pairwise potential is performed at a fixed temperature and vanishing external pressure. As the temperature is increased, a solid-to-liquid transition occurs. When the melting temperature  $T_c$  is approached from below, there is a proliferation of dislocation pairs and the elastic constant approaches the value predicted by the KTHNY theory. In addition, as  $T_c$  is approached from above, the relaxation time increases, consistent with an approach to criticality. However, simulations fail to produce a stable hexatic phase using systems with up to 90,000 particles. A significant jump in enthalpy at  $T_c$  is observed, consistent with either a first order or a continuous transition. The role of external pressure is discussed.

DOI: [10.1103/PhysRevB.83.174110](https://doi.org/10.1103/PhysRevB.83.174110)

PACS number(s): 64.60.A—, 64.70.dm

### I. INTRODUCTION

Melting of an infinite solid in two dimensions has been described as a process driven by a proliferation of thermally excited dislocation pairs in the Kosterlitz-Thouless-Halperin-Nelson-Young (KTHNY) theory.<sup>1–4</sup> The theory, formulated at vanishing external pressure, predicts the existence of a new, “hexatic,” intermediate thermodynamic phase. While solids are characterized by long-range translational and orientational order, liquids present only short-range order. The predicted hexatic phase presents long-range orientational order but lacks long-range translational order. The KTHNY theory predicts a second-order phase transition from the crystalline to the hexatic phase, at which point there is a universal jump of a normalized elastic constant from a finite value to 0. This first transition is followed by a second transition from the hexatic phase to the liquid phase at a higher temperature. The KTHNY theory continues to generate interest, especially because increased numerical capabilities and new experimental techniques currently allow for new and more accurate testing of theoretical predictions. Indeed, there have been numerous attempts at the verification, both experimentally and numerically, of the KTHNY theoretical predictions, with mixed outcomes.

On the experimental side, studies with colloidal particles have provided evidence of two-stage melting with an intermediate hexatic phase<sup>5–8</sup> and of elasticity behavior in agreement with the KTHNY predictions.<sup>9</sup> The observed transition, however, appears to be first order.<sup>8,10</sup> Similar results have been obtained with diblock copolymers.<sup>11</sup> Recently, melting in two steps with an intermediate hexatic phase has been observed in monolayers of polycrystalline colloidal films, but not in thin or thick multilayer films.<sup>12</sup> Also recently, but in a different context, dislocations have been directly observed in graphene,<sup>13</sup> prompting a renewed interest in the role of defects in this two-dimensional material.<sup>14–18</sup>

On the numerical side, molecular dynamics (MD) and Monte Carlo simulations<sup>19,20</sup> of systems with a small number

of particles ( $N$ ) broadly detected a transition where the number of dislocations proliferates but failed to provide clear evidence of the nature of the observed transition. First-order melting has been reported in the literature,<sup>19,21–23</sup> while other calculations support a continuous transition.<sup>24,25</sup>

The critical properties of the KTHNY transition are a consequence of the renormalization effect that small-scale fluctuations have on large-scale fluctuations. For this mechanism to be operative, well-separated length scales must exist, suggesting a minimum size for numerical simulations in two dimensions of  $10^4$ . Indeed, Chen *et al.*<sup>26</sup> performed MD simulations of a Lennard-Jones (LJ) system with a varying number  $N$  of particles. They found a metastable hexatic phase for systems with  $N \geq 36\,864$ , but not for  $N \leq 16\,386$ . In all cases, simulations were performed at a significant external pressure, a fact that alters the dislocation generation mechanism: the interaction between the components of a dislocation pair tends to close it down, while the external pressure, for some orientations, tends to open it up. The whole process becomes one of thermal activation, much like nucleation, and the likelihood of having isolated dislocations—and an hexatic phase—increases. A subsequent study in terms of inherent structure theory showed consistency with the KTHNY theory.<sup>27</sup> More recently, a MD study<sup>28</sup> carried out at a constant volume, involving 36 000 particles interacting through an LJ potential also reported the presence of an hexatic phase between the solid and the liquid phases. However, phase coexistence in NVT ensembles precludes unambiguous interpretation of these results.

In a different vein, in a three-dimensional continuum elastic solid, dislocation loops drive a mechanical instability at a finite temperature,<sup>29,30</sup> at which point the shear modulus vanishes as a function of reduced temperature, following a power law with an exponent whose value is a function that is independent of the microscopic details of the elastic solid. Numerical calculations of superheated LJ crystals near the melting transition in three dimensions show the appearance of dislocations as the temperature is raised.<sup>31,32</sup> However, it is unclear whether these

dislocations play a central role during the phase transition or are just a by-product of another transition-driving mechanism.

The present work used MD simulations in the  $NpT$  ensemble to study the melting transition in two dimensions. MD has been chosen on this occasion over the possible Monte Carlo alternative in order to study the time evolution of the system, especially its relaxation behavior near criticality. We found a single-step solid-to-liquid transition (as determined by the enthalpy change) when a vanishing external pressure was applied to the system, in contrast to a multistep transition at high pressure like the one presented in Ref. 26 using the same number of particles. However, within a narrow temperature interval defining the solid-to-liquid transition, the monitored relaxation times, elastic constants, and evolution of the number of dislocations were all consistent with the KTHNY theory. We suggest that, because of the necessary interplay between many length scales, a stable hexatic phase will be unambiguously observed only in systems with at least  $\sim 10^6$  particles at zero external pressure.

## II. MOLECULAR DYNAMICS SIMULATIONS

MD simulations were carried out using a parallel MD code developed “in house” based on the libraries presented in Ref. 35. Simulation systems comprised  $N$  identical particles of mass  $m$  in two dimensions interacting through a pairwise truncated and shifted LJ potential,

$$\phi_{\text{LJ}}(r) = 4\epsilon \left[ \left( \frac{\sigma}{r} \right)^{12} - \left( \frac{\sigma}{r} \right)^6 \right] - C, \quad (1)$$

for interparticle distances  $r$  smaller than a cutoff radius  $r_c$  and 0 for  $r \geq r_c$ . The value of  $C$  was chosen to ensure continuity of the potential. All simulations were performed using periodic boundary conditions with a fully flexible cell in the  $NpT$  ensemble defined by the non-Hamiltonian equations of motion described by Martyna, Tobias, and Klein.<sup>36</sup> The equations of motion were integrated using the five-value Gear predictor-corrector algorithm.

All simulation parameters and monitored quantities are expressed in reduced units:  $x = x^*\sigma$ ;  $t = t^*\sqrt{m\sigma^2/\epsilon}$ ;  $T = T^*\epsilon/k_B$ , where  $k_B$  is the Boltzmann constant;  $E = E^*\epsilon$ ; and  $p = p^*\epsilon/\sigma^3$  (in the case of argon,  $\epsilon = 0.0104$  eV and  $\sigma = 3.4$  Å, leading to the unit of temperature  $T$  being 120.6 K and the unit of pressure  $p$  being 42 MPa). The integration time step was set to  $0.0005\sqrt{m\sigma^2/\epsilon}$  (34 fs for argon),<sup>26</sup> ensuring extended-energy conservation to 0.005% per million iterations. We also verified momentum conservation and monitored pressure and temperature throughout the simulations. Thermostat and barostat frequencies  $\omega_p$  and  $\omega_b$ <sup>36</sup> were set to values between 80 and 100 and between 0.1 and 0.4, respectively. The cutoff radius was set to 4 and a Verlet-neighbors list was used with a radius of 5.9.

Initial conditions were set by initial positions corresponding to a perfect triangular lattice or a perfect triangular lattice plus a randomly oriented displacement of 0.05 LJ unit, as well as initial velocities given by a Gaussian distribution corresponding to each temperature (initial condition IC1). Otherwise, initial conditions were assigned by equilibrium values of positions and velocities obtained from a previous run

with similar values of  $T$  and  $p$  (initial condition IC2). Most runs were carried out with  $N = 36\,864$ , with up to  $1.7 \times 10^7$  time iterations, and a smaller number of runs with  $N = 90\,000$ .

To characterize the state of the system throughout simulations we monitored the time evolution of the system’s enthalpy and computed the pair and orientational correlation functions  $g(r)$  and  $g_6(r)$ , respectively.<sup>26</sup> The Lamé parameters were also computed, as a function of temperature. The number of dislocation pairs present in the crystal below the transition was examined by counting the number of nearest neighbors for each particle and through visualization with the aid of a Voronoi construction.

## III. RESULTS

### A. Simulations at different temperatures show a melting transition

Two sets of simulations were performed to study the melting behavior of an LJ system. The first set of simulations, aimed at reproducing the results presented in Ref. 26, were performed at  $p = 20$  with  $N = 36\,864$ . Three simulations, performed at temperatures  $T_1 = 2.15$ ,  $T_2 = 2.16$ , and  $T_3 = 2.17$ , were carried out using a perfect crystalline lattice as the initial condition. Despite the use of a different set of equations of motion that are modularly invariant, we obtained results that are consistent with those presented in Ref. 26. The enthalpy  $h$  as a function of time remained stable during the simulation at  $T_1$ , increased rapidly in an apparent single step to achieve a stable value during the simulation performed at  $T_3$ , and increased in two steps with a transient state in the simulation performed at temperature  $T_2$  (data not shown). The pair and orientational correlations functions,  $g(r)$  and  $g_6(r)$ , were consistent with a solid phase for the simulation performed at  $T_1$  and with a liquid phase at the end of simulations performed at  $T_2$  and  $T_3$ . The transient state observed at  $T_2$  exhibits long-range orientational but not translational order, consistent with an hexatic phase. Similar results were obtained with a simulation performed at  $T_2 = 2.16$  that used a thermalized (at  $T = 2.15$ ) set of initial conditions. These results show the possible existence of a metastable and transient hexatic phase when simulations are performed at a high external pressure,  $p = 20$ , as presented in Ref. 26.

To test the behavior of the system at a vanishing external pressure, we performed a second set of simulations in which a system with  $N = 36\,864$  particles starting from initial conditions IC1 and IC2 was simulated at several different temperatures and pressure  $p = 0$  (more precisely, with vanishing normal and tangential stresses). As with the first set of simulations, the enthalpy  $h$  of the system as a function of time (Fig. 1) was stable at low temperatures ( $T \leq 0.40725$ ) but increased in an apparent single-step transition to an equilibrium value for high temperatures ( $T \geq 0.4095$ ). The nature of the phase was characterized using  $g(r)$  and  $g_6(r)$  at the ending configurations of each simulation, confirming a liquid phase for  $T \geq 0.4095$  and a solid phase for  $T \leq 0.40725$  (Fig. 2). As opposed to the results obtained at  $p = 20$ , no intermediate and transient state (possibly corresponding to an hexatic phase) was observed. It is possible that an hexatic phase with an algebraically decaying  $g_6(r)$  and an exponentially decaying

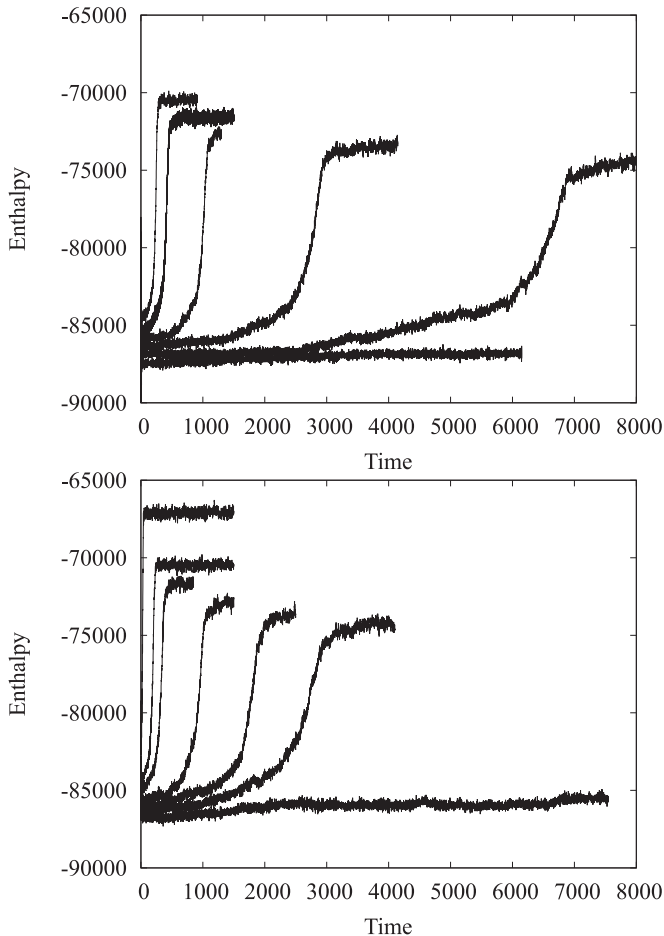


FIG. 1. Enthalpy as a function of time for several temperatures. Top: Initial conditions are given by initial positions corresponding to a perfect triangular lattice plus a randomly oriented displacement of 0.05 LJ unit, and initial velocities are given by a Gaussian distribution corresponding to each temperature (initial condition IC1). From the bottom-right to the top-left curves, the temperatures are  $T = 0.4050, 0.4095, 0.4130, 0.4160, 0.4200, \text{ and } 0.4250$ . Bottom: Positions and velocities are provided, at each temperature, by the equilibrium values obtained in a previous run at  $T = 0.40725$  (initial condition IC2). From the bottom-right to the top-left curves the temperatures are  $T = 0.40725, 0.41000, 0.41250, 0.41500, 0.42000, 0.42500, \text{ and } 0.44000$ . All simulations were carried out at vanishing external pressure.

$g(r)$  could be found within the interval of temperatures given by  $T_- = 0.40725 < T < T_+ = 0.4095$ . However, it was not possible to reach equilibrium in between these two temperature values within the available simulation time scales (data not shown). Defining the relative change in enthalpy as  $\Delta h \equiv 2(h_+ - h_-)/(h_+ + h_-)$  [where  $h_{\pm} \equiv h(T_{\pm})$ ] and the relative change in temperature as  $\Delta T \equiv 2(T_+ - T_-)/(T_+ + T_-)$ , we find  $\Delta h = 0.1433$  and  $\Delta T = 0.0044$ . Within this narrow temperature interval, our data are consistent both with an abrupt jump from a low to a high enthalpy value at some intermediate temperature, as would be the case for a first-order transition (i.e., with latent heat), and with a two-step change of enthalpy as a function of temperature within the temperature interval, as would be the case for a continuous transition, without latent heat (Fig. 3).

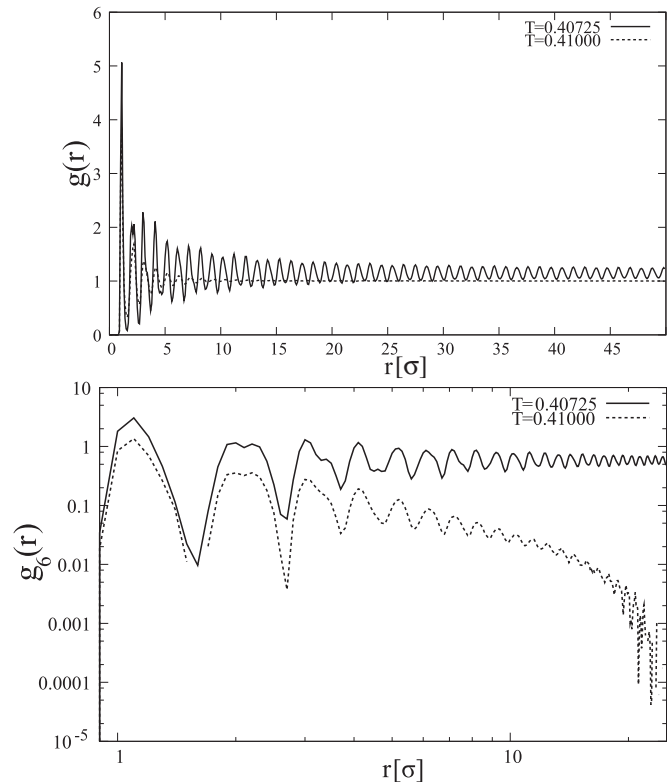


FIG. 2. Top: The pair correlation function at  $T = 0.40725$  indicates long-range translational order; at  $T = 0.41000$ , the absence of it. Bottom: Orientational correlation function at  $T = 0.40725$  indicates long-range order; at  $T = 0.41000$ , the lack of it.

**B. Relaxation times slightly above melting increase as the melting temperature is approached**

Near a critical point, relaxation times increase as criticality is approached. This is due to the increasing size of fluctuations,<sup>37</sup> which reach macroscopic dimensions at the

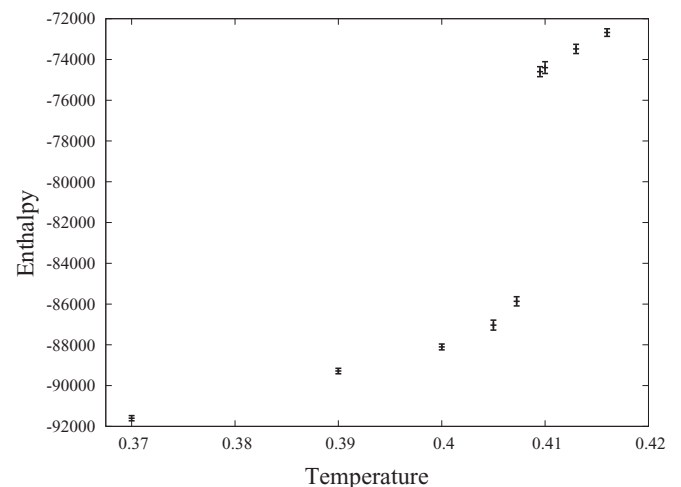


FIG. 3. Final enthalpy as a function of temperature. It shows a significant increase at  $T_c = 0.40815 \pm 0.00090$ . The low-temperature phase is a solid, as evidenced by the behavior of pair and orientational correlation functions. The high-temperature phase is a liquid (Figure 2).

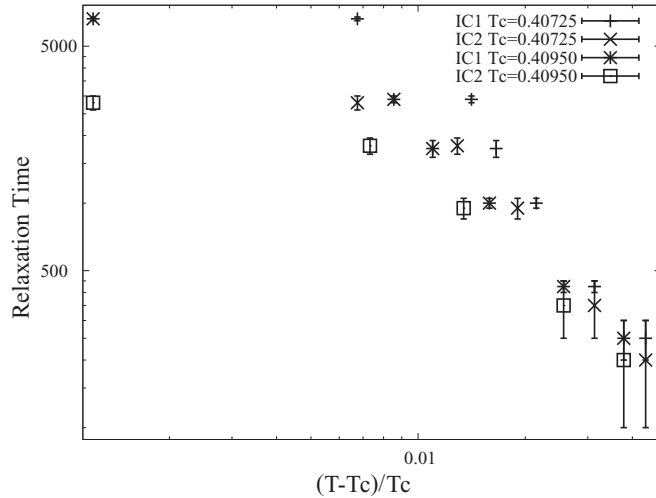


FIG. 4. Relaxation time as a function of temperature as the transition temperature  $T_c$  is approached from above. There are four sets of points, corresponding to the two different initial conditions (IC1 and IC2) indicated in Fig. 1, and two possible values of  $T_c$ , determined by the finite interval in which  $T_c$  is found. The time increases without limit as  $T_c$  is approached, consistent with criticality. Error bars are given by  $t_{\min} - t_{\max}$ .

critical point. To determine the nature of the phase transition observed at  $p = 0$ , we monitored the relaxation time ( $t_R$ ) as a function of temperature in the simulations mentioned at  $T > T_c$  (Fig. 4).

The relaxation time  $t_R$  is defined, grossly, as the instant where the second derivative of enthalpy vs time vanishes and, more precisely, as follows: the enthalpy-vs-time curve is interpolated by a smooth function whose second derivative is computed numerically, and the times  $t_{\max}$ , where curvature is a maximum, and  $t_{\min}$ , where it is a minimum, are determined. The relaxation time is then defined through  $t_R = t_{\max} + (t_{\min} - t_{\max})/2$ .

Within the accuracy of the simulation, this time grows without limit as the melting temperature is approached, consistent with an approach to criticality and a second-order phase transition. The range of values that was explored, however, was not large enough to detect a possible power-law behavior. These results did not depend on the initial conditions used (IC1 or IC2) or on the critical temperature used [ $T_c = 0.40725$  or  $T_c = 0.4095$ , as there is no exact melting temperature but rather an interval ( $T_-, T_+$ )].

### C. Behavior of elastic constants is consistent with KTHNY theory

Another way to determine the nature of the phase transition at  $p = 0$  and whether it is consistent with theoretical predictions consists of monitoring the behavior of the elastic constants of the system. The elastic response of an isotropic, homogeneous, continuum solid is characterized by two Lamé coefficients,  $\lambda$  and  $\mu$ . They appear in the compliance tensor as

$$S_{ijkl} = \frac{1}{4\mu} \left( \delta_{ik}\delta_{jl} + \delta_{il}\delta_{jk} - \frac{\lambda}{\lambda + \mu} \delta_{ij}\delta_{kl} \right), \quad (2)$$

where

$$\epsilon_{ij} = S_{ijkl}\sigma_{kl},$$

$\epsilon_{ij}$  is the strain, and  $\sigma_{kl}$  the stress. There are several possible ways to extract  $\lambda$  and  $\mu$  from this tensor. In the continuum theory they are, of course, equivalent. But in a numerical calculation involving a finite number of atoms, this will no longer necessarily be the case. They should coincide, however, within the numerical accuracy and error bars (see below). The following relations hold for the combination of Lamé coefficients:

$$K \equiv \frac{4\mu(\lambda + \mu)}{2\mu + \lambda} \quad (3)$$

$$= \frac{1}{S_{0000}} \equiv K_1 \quad (4)$$

$$= \frac{1}{S_{1111}} \equiv K_2 \quad (5)$$

$$= \frac{1}{S_{0011} + 2S_{0101}} \equiv K_3. \quad (6)$$

It is a significant prediction of the KTHNY theory that  $K$  approaches a universal value as the critical temperature  $T_c$  is approached from below:

$$\lim_{T \rightarrow T_c^-} K = 16\pi \frac{k_B T_c}{b^2} \equiv K_c, \quad (7)$$

where  $b$  is the Burgers vector of the dislocations (given by the lattice constant at zero temperature).  $K$  vanishes above  $T_c$ .

We have computed the strain of our system following Ray and Rahman,<sup>39,40</sup>

$$\epsilon = \frac{1}{2} \left[ (\mathbf{h}_R^{-1})^t \mathbf{h}' \mathbf{h} \mathbf{h}_R^{-1} - \mathbf{I} \right], \quad (8)$$

where  $\mathbf{h}$  is a  $2 \times 2$  matrix whose column vectors define the simulation box,  $\mathbf{h}_R$  is a reference box (here taken as the time average of the simulation box), and  $\mathbf{I}$  is the identity matrix. The compliance tensor is given in terms of strain fluctuations through

$$S_{ijkl} = \beta V_R (\langle \epsilon_{ij} \epsilon_{kl} \rangle - \langle \epsilon_{ij} \rangle \langle \epsilon_{kl} \rangle), \quad (9)$$

where  $V_R$  is the volume of the reference box.

The compliances were calculated from simulations of  $2.5 \times 10^6$  time steps, after  $5 \times 10^5$  equilibration steps. The error bars were estimated by performing blocking averages<sup>33,34</sup> and then propagating the error in Eq. (9). The simulation data were divided into five data blocks. The value of the Burgers vector was estimated as the lattice constant that minimizes

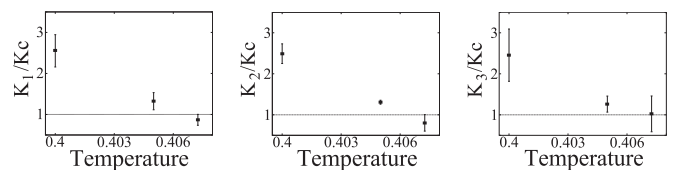


FIG. 5. Elastic constant  $K_1/K_c$  (left),  $K_2/K_c$  (middle), and  $K_3/K_c$  (right) as a function of temperature. Within numerical accuracy they coincide, as they should. Near the transition their value is consistent with 1, as predicted by the KTHNY theory.

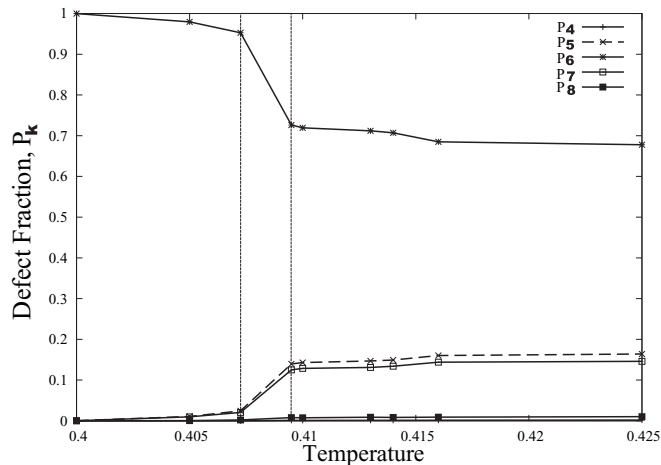


FIG. 6.  $P_k$ , the fractional number of sites with  $k$  neighbors, as a function of temperature for  $k = 4, 5, 6, 7, 8$ . There is a significant decrease in  $P_6$  across the solid-liquid transition, with a corresponding increase in  $P_5$  and  $P_7$ , consistent with a transition driven by the unbinding of dislocation pairs.

the energy of a triangular crystal,  $b_0 = 1.11145\sigma$ . Figure 5 shows the ratios  $K_1/K_c$ ,  $K_2/K_c$ , and  $K_3/K_c$  as a function of temperature as the transition is approached from below. The computed values are consistent with the KTHNY theory.

#### D. Proliferation of dislocations is consistent with KTHNY theory

Finally, and to fully characterize the transition observed at  $p = 0$ , we monitored the number of dislocations as a function of temperature, counting the number of neighbors for each point using a Voronoi construction after equilibrium had been reached. Figure 6 shows  $P_k$ , the fractional number of sites with  $k$  neighbors, as a function of temperature. Of course, for a perfect triangular lattice,  $P_6 = 1$  and  $P_k = 0$  for  $n \neq 6$ . A dislocation is characterized by two neighboring sites, one with five and the other with seven neighbors. The KTHNY theory predicts that the loss of long-range translational order is due to the proliferation, and subsequent unbinding, of thermally generated dislocation pairs. Such pairs will be characterized then by clusters of four sites, two of them with five and two of them with seven neighbors. Figure 6 shows that across the solid-to-liquid transition there is a significant decrease in  $P_6$ , and a corresponding increase in  $P_5$  and  $P_7$ , consistent with the KTHNY theory.

Figure 7 also provides a visual illustration of the number of dislocations, monitored with the number of sites having five or seven nearest neighbors, within the simulation box for different temperatures. Their proliferation is apparent, consistent with the KTHNY theory.

#### IV. DISCUSSION: THE ROLE OF EXTERNAL PRESSURE

An hexatic phase has been observed in simulations presented by Chen *et al.*<sup>26</sup> and also reproduced here. However, this phase is transient, not in equilibrium, and occurs when the LJ is subjected to the significant external pressure of 20. The

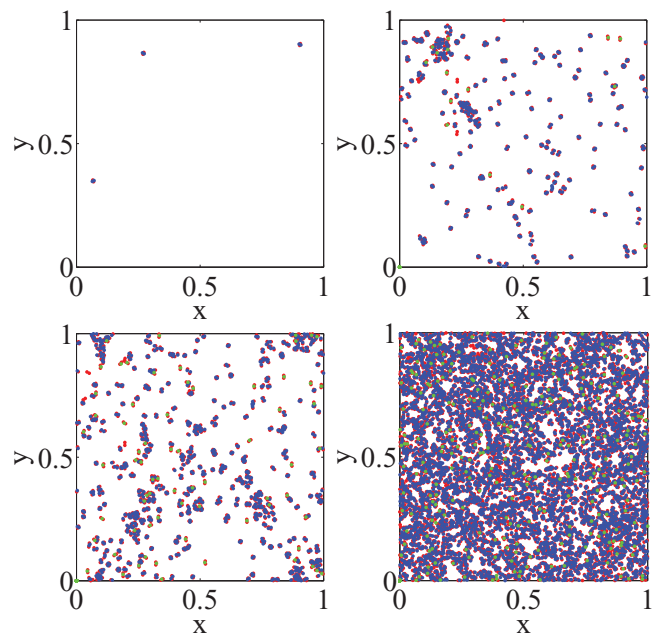


FIG. 7. (Color online) Dislocation dipole population as a function of temperature, monitored with the sites having five (red) and seven (blue) neighbors. Top left,  $T = 0.400$ ; top right,  $T = 0.405$ ; bottom left,  $T = 0.40725$ ; all three temperature values below  $T_c$ . Bottom right:  $T = 0.4095$ , just above  $T_c$ . The number of dislocation dipoles steadily increases as the transition is approached. Sites with eight neighbors (green) are also indicated.

use of a constant-pressure ensemble MD ensures the existence of a homogeneous phase. However, we have been unable to observe the hexatic phase at a constant vanishing external pressure. Is there a reason, within the KTHNY theory, not to observe an hexatic phase at zero external pressure with a finite number of particles?

The hexatic phase arises<sup>2</sup> after (i.e., at a higher temperature) a triangular lattice undergoes a dislocation unbinding transition but before (i.e., at a lower temperature) a disclination unbinding transition occurs. The latter is possible because the plasma of free dislocations screens the disclination-disclination interaction, allowing a transition much like the one originally considered by Kosterlitz and Thouless.<sup>1</sup> As mentioned in Sec. I, it is critical, in a numerical simulation, to have several length scales available, since the KTHNY mechanism involves the interaction among defects of different sizes, at many scales. This is in addition to the fact that the theoretical analysis is carried out in the thermodynamic limit. We now argue that at least  $10^6$  particles are needed in simulations, to have three decades in length scales.

The physics of dislocation unbinding changes considerably when an external pressure  $p$  is included. Indeed, the energy  $U$  of a dislocation dipole with Burgers vector  $\vec{b}$ , whose components are separated by  $\vec{R}$  in this case, is<sup>38</sup>

$$U(R) = \frac{b^2 K}{4\pi} \left[ \log \left( \frac{R}{\tau} \right) + C - \frac{1}{2} \cos 2\theta \right] + P b R \sin \theta, \quad (10)$$

where  $\tau$  is the dislocation core size;  $\mathcal{C}$ , roughly, determines the core energy (i.e., the minimum energy needed to generate a dipole);  $R = |\vec{R}|$ ;  $b = |\vec{b}|$ ; and  $\theta$  is the angle between  $\vec{R}$  and  $\vec{b}$ . Clearly, when  $\sin \theta < 0$  the last term on the right-hand side turns the dislocation-dipole unbinding process into a thermally activated one, with an activation energy  $U_A$  (taking  $\theta = -\pi/2$ , the most favorable case, for illustration purposes):

$$U_A \equiv \frac{b^2 K}{4\pi} \left[ \log \left( \frac{1}{4\pi} \frac{K b}{P \tau} \right) + \mathcal{C} - \frac{1}{2} \right].$$

Consequently, and given the logarithmic dependence on the ratio of external pressure to elastic constant, even a modest value of external pressure  $P$ , compared to  $K$ , will give values for the activation energy in the same ballpark as the chemical potential for the dislocation dipole, and a proliferation of isolated dislocations will ensue. Thus, it will not be surprising in those circumstances to observe an hexatic phase. However, Eq. (10) shows that, at any given nonvanishing pressure, there will be a finite rate of dislocation generation, driving the system away from equilibrium. A quantitative study of this interesting phenomenon is outside the scope of the present paper.

In the absence of external pressure, disclination pairs above the dislocation unbinding transition interact via an energy that depends on the logarithm of their mutual distance, with a coupling (called  $K_A$  by Nelson and Halperin)<sup>2</sup> that is finite due to the screening effect of the free dislocations. A second transition toward the liquid state thus occurs because of two distinct screenings: free dislocations screen the interaction between disclination pairs to an effective logarithmic interaction, and then this interaction is renormalized because of the interaction between disclination pairs at different length scales. So, three length scales should be needed for this scale-dependent interaction among disclination pairs to become operative. In addition, a further length scale would seem to be necessary to have enough free dislocations in between a disclination pair for their interaction to be effectively screened. According to this reasoning, at least  $\sim 10^6$  particles would be needed

to observe an hexatic phase as an equilibrium phase at zero external pressure in a numerical simulation.

## V. CONCLUSIONS

The KTNHY theory of melting in two dimensions<sup>1-3</sup> involves the interaction among dislocation dipoles whose sizes span different length scales. Thus, a numerical simulation that aims at verifying the theory should involve enough different length scales for this interaction to be possible. In two dimensions,  $10^4$  particles thus appears to be the absolute minimum. Increasing this number should improve the statistics. By the same token,  $10^6$  particles should be a minimum number to capture this type of effect in three dimensions. Our simulation has been carried at constant (vanishing) external pressure to prevent phase coexistence. We find a solid-to-liquid transition, and the behavior of the solid phase as the transition temperature is approached is consistent with the predictions of KTNHY. The behavior of enthalpy as a function of temperature is less conclusive: it changes significantly across a narrow temperature range  $\Delta T$ , from a solid low-temperature phase to a liquid high-temperature phase. The behavior within  $\Delta T$  could not be resolved because of the limited time scale that can be reached with simulations. There could be an abrupt discontinuity, as in a first-order transition, or there could be a smooth change, including a temperature range with an hexatic phase. Above  $T_c$ , the relaxation time increases as  $T_c$  is approached, consistent with criticality.

## ACKNOWLEDGMENTS

We thank Rodrigo Arias and Patricio Cordero for useful discussions. This work was supported by Fondecyt Grant Nos. 1100100 and 1100198, Fondap Grant No. 11980002, Anillo ACT 127, and a Conicyt 2002 fellowship (to M.S.). M.S. is a Howard Hughes Medical Institute Fellow of the Helen Hay Whitney Foundation.

\*Corresponding author: flund@cimat.cl

<sup>1</sup>J. M. Kosterlitz and D. J. Thouless, *J. Phys. C* **6**, 1181 (1973).

<sup>2</sup>B. I. Halperin and D. R. Nelson, *Phys. Rev. Lett.* **41**, 121 (1978); D. R. Nelson and B. I. Halperin, *Phys. Rev. B* **19**, 2457 (1979).

<sup>3</sup>A. P. Young, *Phys. Rev. B* **19**, 1855 (1979).

<sup>4</sup>D. R. Nelson, *Defects and Geometry in Condensed Matter Physics* (Cambridge University Press, Cambridge, 2002).

<sup>5</sup>C. A. Murray and D. H. Van Winkle, *Phys. Rev. Lett.* **58**, 1200 (1987).

<sup>6</sup>R. E. Kusner, J. A. Mann, J. Kerins, and A. J. Dahm, *Phys. Rev. Lett.* **73**, 3113 (1994).

<sup>7</sup>K. Zahn, R. Lenke, and G. Maret, *Phys. Rev. Lett.* **82**, 2721 (1999).

<sup>8</sup>B.-J. Lin and L.-J. Chen, *J. Chem. Phys.* **126**, 034706 (2007).

<sup>9</sup>H. H. von Grünberg, P. Keim, K. Zahn, and G. Maret, *Phys. Rev. Lett.* **93**, 255703 (2004).

<sup>10</sup>A. H. Marcus and S. A. Rice, *Phys. Rev. Lett.* **77**, 2577 (1996).

<sup>11</sup>D. E. Angelescu, C. K. Harrison, M. L. Trawick, R. A. Register, and P. M. Chaikin, *Phys. Rev. Lett.* **95**, 025702 (2005).

<sup>12</sup>Y. Peng, Z. Wang, A. M. Alsayed, A. G. Yodth, and Y. Han, *Phys. Rev. Lett.* **104**, 205703 (2010).

<sup>13</sup>A. Hashimoto, K. Suenaga, A. Gloter, K. Urita, and S. Iijima, *Nature* **430**, 870 (2004).

<sup>14</sup>A. Carpio, L. L. Bonilla, F. de Juan, and M. A. H. Vozmediano, *New J. Phys.* **10**, 053021 (2008).

<sup>15</sup>B. W. Jeong, J. Ihm, and G.-D. Lee, *Phys. Rev. B* **78**, 165403 (2008).

<sup>16</sup>A. Mesaros, D. Sadri, and J. Zaanen, *Phys. Rev. B* **79**, 155111 (2009).

<sup>17</sup>E. Ertekin, D. C. Chrzan, and M. S. Daw, *Phys. Rev. B* **79**, 155421 (2009).

<sup>18</sup>O. V. Yazyev and S. G. Louie, *Phys. Rev. B* **81**, 195420 (2010).

<sup>19</sup>S. Toxvaerd, *Phys. Rev. A* **24**, 2735 (1981).

<sup>20</sup>M. P. Allen, D. Frenkel, W. Gignac, and J. P. McTague, *J. Chem. Phys.* **78**, 4206 (1983).

<sup>21</sup>K. J. Strandburg, J. A. Zollweg, and G. V. Chester, *Phys. Rev. B* **30**, 2755 (1984).

- <sup>22</sup>A. F. Bakker, C. Bruin, and H. J. Hilhorst, *Phys. Rev. Lett.* **52**, 449 (1984).
- <sup>23</sup>J. Lee and K. J. Strandburg, *Phys. Rev. B* **46**, 11190 (1992).
- <sup>24</sup>M. Li, *Phys. Rev. B* **62**, 13979 (2000).
- <sup>25</sup>J. F. Fernández, J. J. Alonso, and J. Stankiewicz, *Phys. Rev. E* **55**, 750 (1997).
- <sup>26</sup>K. Chen, T. Kaplan, and M. Mostoller, *Phys. Rev. Lett.* **74**, 4019 (1995).
- <sup>27</sup>F. L. Somer, G. S. Canright, T. Kaplan, K. Chen, and M. Mostoller, *Phys. Rev. Lett.* **79**, 3431 (1997); F. L. Somer, G. S. Canright, and T. Kaplan, *Phys. Rev. E* **58**, 5748 (1998).
- <sup>28</sup>H. Shiba, A. Onuki, and T. Araki, *Europhys. Lett.* **86**, 66004 (2009).
- <sup>29</sup>F. Lund, *Phys. Rev. Lett.* **69**, 3084 (1992).
- <sup>30</sup>R. Arias and F. Lund, *Defect Diffus. Forum* **150–151**, 121 (1997).
- <sup>31</sup>Z. H. Jin, P. Gumbsch, K. Lu, and E. Ma, *Phys. Rev. Lett.* **87**, 055703 (2001).
- <sup>32</sup>L. Gómez, A. Dobry, Ch. Geuting, H. T. Diep, and L. Burakovsky, *Phys. Rev. Lett.* **90**, 095701 (2003).
- <sup>33</sup>D. Frenkel and B. Smit, *Understanding Molecular Simulation: From Algorithms to Applications* (Academic Press, New York, 2002).
- <sup>34</sup>W. Janke, in *Quantum Simulations of Complex Many-Body Systems: From Theory to Algorithms, NIC Series, Vol. 10*, edited by J. Grotendorst, D. Marx, and A. Muramatsu (John von Neumann Institute for Computing, Juelich, 2002).
- <sup>35</sup>M. P. Allen and D. J. Tildesley, *Computer Simulations of Liquids* (Oxford Science, New York, 1987).
- <sup>36</sup>G. J. Martyna, D. J. Tobias, and M. L. Klein, *J. Chem. Phys.* **101**, 4177 (1994).
- <sup>37</sup>P. C. Hohenberg and B. I. Halperin, *Rev. Mod. Phys.* **49**, 436 (1977).
- <sup>38</sup>J. P. Hirth and J. Lothe, *Theory of Dislocations* (Krieger, Malabar, FL, 1992).
- <sup>39</sup>J. R. Ray, *J. Appl. Phys.* **53**, 6441 (1982).
- <sup>40</sup>J. R. Ray and A. Rahman, *J. Chem. Phys.* **80**, 4423 (1984).